Thermochimica Acta 486 (2009) 57–65

Contents lists available at ScienceDirect

Thermochimica Acta

journal homepage: www.elsevier.com/locate/tca

Heat capacities of several Al–Ni–Ti compounds

Rongxiang Hu [a], Philip Nash [a,*], Qing Chen [b], Lijun Zhang [c], Yong Du [c]

[a] Thermal Processing Technology Center, Illinois Institute of Technology, 10 West 32nd St., Chicago, IL 60616, USA
[b] Thermo-Calc Software AB, Björnnäsvägen 21, 113 47 Stockholm, Sweden
[c] State Key Laboratory of Powder Metallurgy, Central South University, Hunan, 410083, PR China

ARTICLE INFO

Article history:
Received 18 September 2008
Received in revised form
14 November 2008
Accepted 5 December 2008
Available online 31 December 2008

Keywords:
Heat capacity
Drop calorimetry
Al–Ni–Ti alloys

ABSTRACT

The heat capacities of several Al–Ni–Ti compounds were determined by drop calorimetry over the temperature range of 500–1500 K. A modified Einstein model and a two-parameter polynomial model provide reasonable representations of the experimental heat capacity data. The heat capacities, C_p, using a two-parameter polynomial representation are as follows: $Ni_{0.5}Ti_{0.5}$, $C_p = 22.39 + 8.24 \times 10^{-3}\,T$ (J/(mol K)); $Al_{0.45}Ni_{0.5}Ti_{0.05}$, $C_p = 23.01 + 5.12 \times 10^{-3}\,T$ (J/(mol K)); $Al_{0.16}Ni_{0.74}Ti_{0.10}$, $C_p = 18.36 + 10.76 \times 10^{-3}\,T$ (J/(mol K)); and $Al_{0.25}Ni_{0.5}Ti_{0.25}$, $C_p = 25.38 + 1.088 \times 10^{-3}\,T$ (J/(mol K)). The experimental data are compared with the values derived from a thermodynamic database of Gibbs energy functions. The analysis shows that (1) either model is a good representation of the data; (2) it is not adequate to assume the Neumann-Kopp rule for the description of the heat capacities of $Al_{0.45}Ni_{0.5}Ti_{0.05}$, $Al_{0.16}Ni_{0.74}Ti_{0.10}$ and $Al_{0.25}Ni_{0.5}Ti_{0.25}$; (3) it is not appropriate to determine a compound C_p from a thermodynamic database of Gibbs energy functions if the compound is modeled by using the Neumann-Kopp rule and any of its components undergoes melting in the temperature range of interest.

1. Introduction

The Al–Ni–Ti system forms the basis for several important alloys: shape memory alloys based on NiTi B2 phase [1], potential structural alloys based on AlNi B2 phase [2], and superalloys based on the γ/γ′ phase equilibrium [3]. The Al–Ni–Ti phase diagram has been the subject of numerous experimental studies of phase equilibria [4–8] and rather less on thermodynamic properties [9,10,11], although thermodynamic data, including the heat capacity, are very important for phase diagram calculation and process simulation. To remedy the situation, this work was performed to provide additional thermodynamic data for thermodynamic modeling of the system.

There are many methods for measuring the heat capacity [12–15]. The method selected in this work was drop calorimetry [16,17]. However, one of the problems associated with experimental determination of heat capacity data is how to represent the data mathematically. There are two models frequently used for representation of the heat capacity data, i.e. modified Einstein model [18] and polynomial model [19]. The experimental data determined in this work were used to compare the two different models, and also compared with the calculated values derived from a thermodynamic database [20] to determine which provides the best representation of the data.

2. Experimental procedure

Ti (99.99%), Al (99.97%), and Ni (99.996%) elemental powders from Alfa Aesar were used to synthesize the samples for the experiments. To remove surface contamination, the Ni powder was reduced in a hydrogen gas furnace immediately before preparing a compact of the elemental powders. Four compositions from different single-phase areas in the Al–Ni–Ti system were selected for the measurement: $Al_{0.45}Ni_{0.5}Ti_{0.05}$, $Ni_{0.5}Ti_{0.5}$, $Al_{0.16}Ni_{0.74}Ti_{0.10}$ and $Al_{0.25}Ni_{0.5}Ti_{0.25}$. For each composition, five samples were prepared by synthesizing the compounds with a Kleppa high temperature calorimeter (HTRC) at 1373 K and their enthalpies of formation were determined, as described in [21]. The enthalpy values obtained are reported in another paper [11]. XRD (X-ray diffraction) was used to verify that the samples were single phase. DTA (differential thermal analysis) was used to determine any transformations occurring in the experimental temperature range. The DTA scan rate between room temperature and 1173 K was 10 K/min and above 1173 K the scan rate was 5 K/min. In order to determine the heat capacities of the Al–Ni–Ti compounds, the heat contents were measured using a Multi-detector High Temperature Calorimeter Ligne 96 (MHTC 96) from Setaram (Lyon, France). The measurements were carried out in the temperature range from 483 to 1500 K at intervals of 100 K in an argon atmosphere. The calorimeter

* Corresponding author. Tel.: +1 3125673056; fax: +1 3125678875.
E-mail address: nash@iit.edu (P. Nash).

0040-6031/$ – see front matter © 2008 Elsevier B.V. All rights reserved.
doi:10.1016/j.tca.2008.12.027

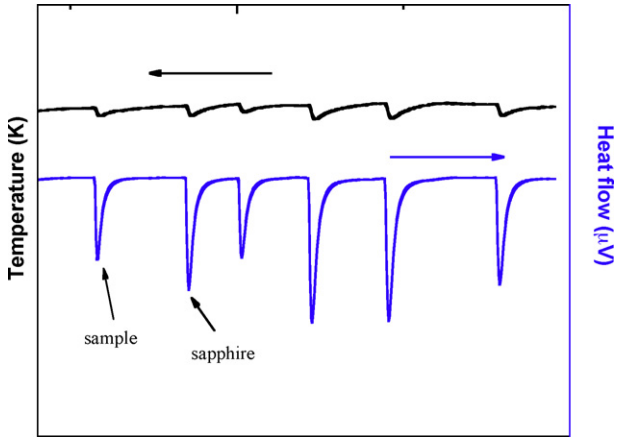

Fig. 1. Example of heat content determination for $Ni_{0.5}Ti_{0.5}$ at 790 K.

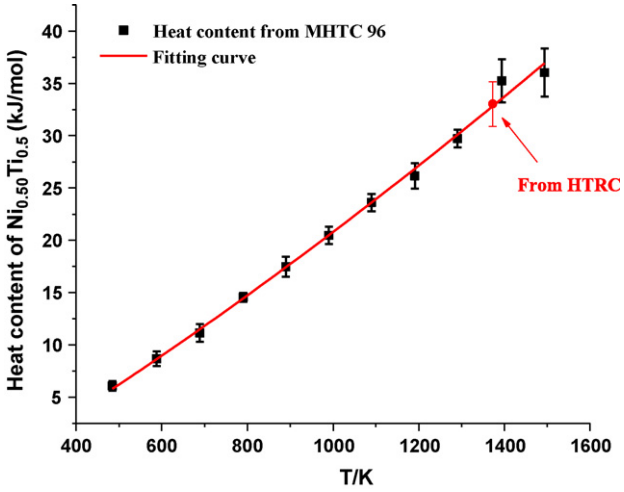

Fig. 3. Heat content of $Ni_{0.5}Ti_{0.5}$.

temperature was calibrated using Zn shot (99.9999%), Ag (99.9%), Au (99.99%), Sn (99.99%) and Al (99.99999%) foils, by comparing their experimental melting points with the standard values. At each temperature, five samples and five references (sapphire, NIST SRM No. 720) were dropped alternately from room temperature into the working cell of the preheated calorimeter. Fig. 1 shows the heat content result for $Ni_{0.5}Ti_{0.5}$ at 790 K. Each peak corresponds to either a sample or a reference. The time interval between peaks is about 20–30 min. The weight of each sample was about 120 mg and the sapphire about 100 mg. Endothermic effects are detected and the relevant peak area $Q(T)$ is proportional to the heat content of the dropped specimen between room temperature (T_0) and the calorimeter temperature (T), i.e. $\Delta H(T)$:

$$Q(T) = K(T)\frac{m}{M}\Delta H(T) = K(T)\int_{T_0}^{T} C_p dT \quad (1)$$

in which $K(T)$ is a calibration coefficient obtained from the sapphire standard reference peaks, m and M are sample weight and molecular mass, respectively. C_p is molar heat capacity.

The precision of the calorimeter was determined by measuring the heat content of Molybdenum (NIST, SRM No.781D2) between room temperature and temperatures in the range of 483–1496 K, as shown in Fig. 2. The obtained values were in excellent agreement with the NIST standard reference data [22]. The maximum deviation is approximately 0.8% from the recommended NIST data.

3. Results and discussion

3.1. Fitting with modified-Einstein model

Chase et al. [18] proposed the modified Einstein model for the description of heat capacities for pure elements or compounds, as expressed in the following equation:

$$C_p = 3R\left(\frac{\Theta_E}{T}\right)^2 \frac{\exp(\Theta_E/T)}{(\exp(\Theta_E/T)-1)^2} + bT + dT^2 + C_p^{\mathrm{mag}} \quad (2)$$

where the first term is the contribution from the harmonic lattice vibrations, and Θ_E is the Einstein temperature; the second term contains the contributions from electronic excitations and low-order anharmonic corrections (dilatational and explicitly anharmonic); the third term is from the high-order anharmonic lattice vibrations; the last term, C_p^{mag}, is an additional term for ferromagnetic compounds. This expression has also been successfully applied in describing the thermodynamic properties of pure iron by Chen and Sundman [23].

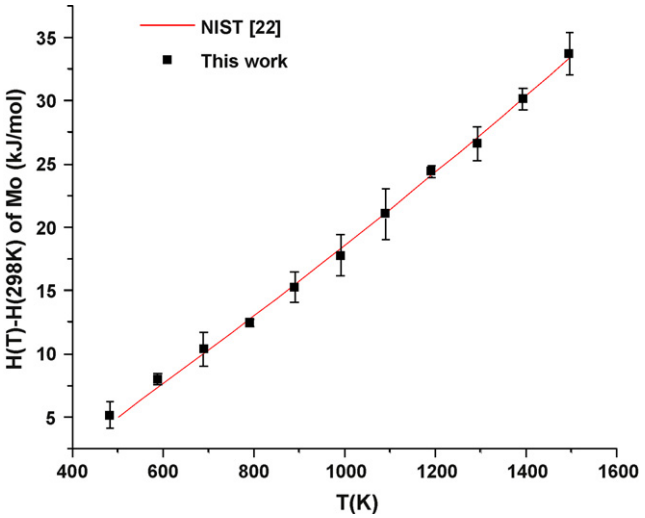

Fig. 2. Heat content of Mo determined in this work and from NIST [22].

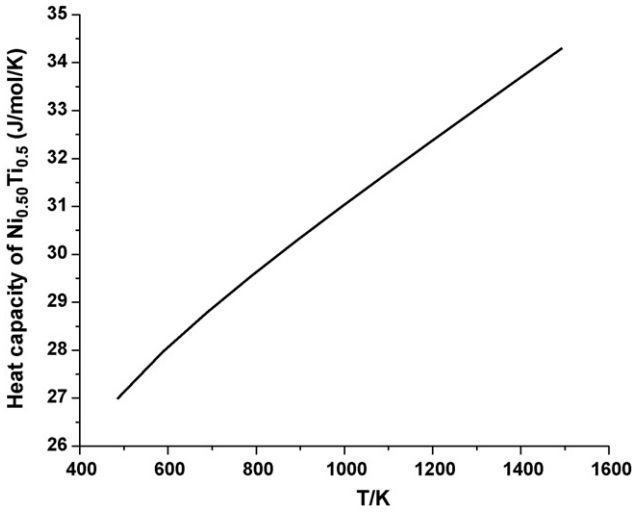

Fig. 4. Molar heat capacity of $Ni_{0.5}Ti_{0.5}$.

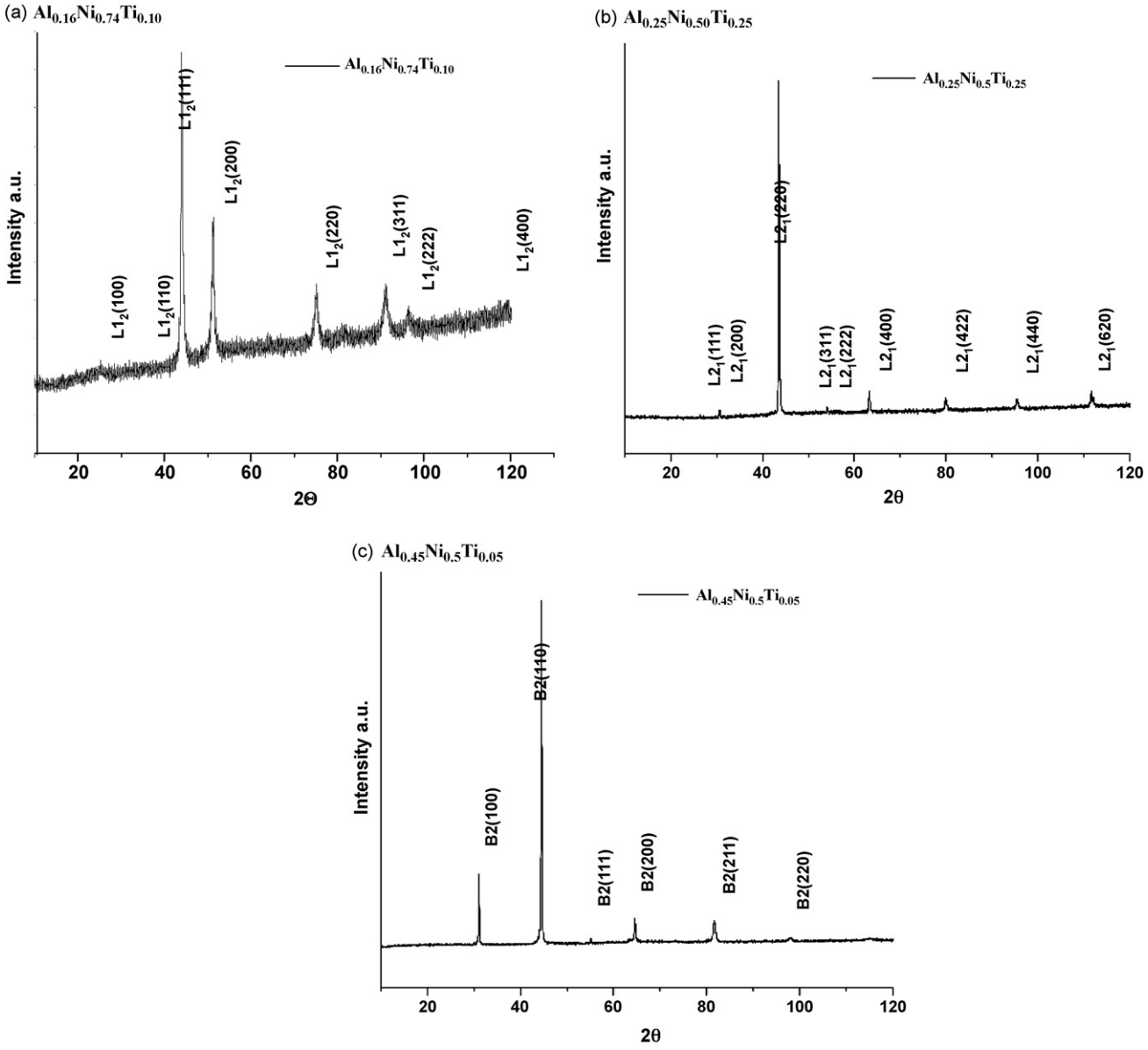

Fig. 5. XRD patterns of Al–Ni–Ti compounds: (a) $Al_{0.16}Ni_{0.74}Ti_{0.10}$; (b) $Al_{0.25}Ni_{0.50}Ti_{0.25}$; (c) $Al_{0.45}Ni_{0.50}Ti_{0.05}$.

After integrating Eq. (2), one obtains the heat content:

$$\Delta H = A + 3R\Theta_E \frac{1}{e^{\Theta_E/T} - 1} + \frac{b}{2}T^2 + \frac{d}{3}T^3 \quad (3)$$

in which A is a constant of integration. This function was used in fitting the experimental data. Although the Einstein temperature in Eq. (3) could be used as a fitting parameter, we preferred to calculate it as described below since no lower temperature specific heat data were determined in our work and when the Einstein temperature was used as a fitting parameter the uncertainty in the fitting was large and unrealistic values were obtained for the other fitting parameters.

3.2. Heat capacity fitting for $Ni_{0.5}Ti_{0.5}$

The Einstein temperature in Eq. (3) can be obtained from the Debye temperature via $\Theta_E = \sqrt[3]{\pi/6} \times \Theta_D$ [24], where Θ_D is the Debye temperature. As discussed by Mitra and Chattopadhyay [25], the Debye temperature of compounds can be calculated from the Debye temperatures of their components based on the Neumann-Kopp rule [26], that is

$$\Theta_D(Ni_{0.5}Ti_{0.5}) = \sqrt{0.5(\Theta_D(Ni))^2 + 0.5(\Theta_D(Ti))^2}$$
$$= \sqrt{0.5 \times 440^2 + 0.5 \times 420^2} = 430\,K$$

$$\Theta_E(Ni_{0.5}Ti_{0.5}) = \sqrt[3]{\frac{\pi}{6}}\Theta_D = 346\,K$$

Using the least squares method, the experimental heat content data of $Ni_{0.5}Ti_{0.5}$ from 298 K to temperatures in the range 481–1393 K were fit using Eq. (3). Differentiating this fit resulted in an unrealistic C_p versus T function. The data were then fit using the reduced form of Eq. (3) by neglecting the term in T^3, this fit is shown in Fig. 3 and the following parameter values are given:

$$\Delta H = 3R \times 346 \times 10^{-3} \frac{1}{\exp(346/T) - 1}$$
$$+3.167 \times 10^{-6}T^2 - 3.23\,(kJ/mol) \quad (4)$$

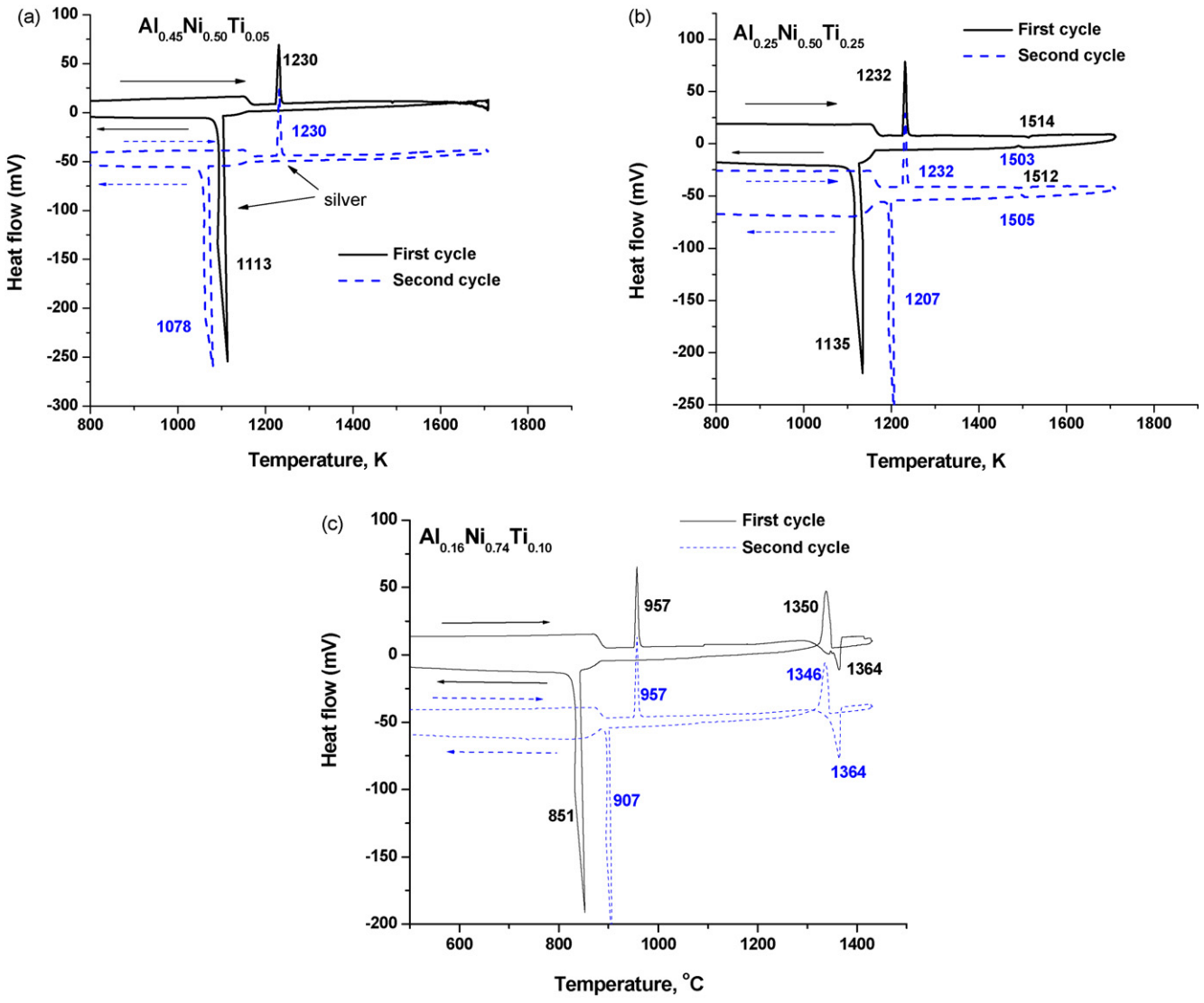

Fig. 6. DTA of Al–Ni–Ti compounds (arrows indicate heating or cooling): (a) $Al_{0.45}Ni_{0.50}Ti_{0.05}$; (b) $Al_{0.25}Ni_{0.50}Ti_{0.25}$; (c) $Al_{0.16}Ni_{0.74}Ti_{0.10}$.

In addition to the heat content data obtained from the MHTC 96, the heat content determined from the High Temperature Reaction Calorimeter (HTRC) is shown and it is in excellent agreement with the results from the MHTC 96.

After differentiating the heat content fit equation, the specific heat capacity of $Ni_{0.5}Ti_{0.5}$ was determined to be

$$C_p = 3R\left(\frac{346}{T}\right)^2 \frac{\exp(346/T)}{(\exp(346/T)-1)^2} + 6.33\times10^{-3}T(\mathrm{J/(mol\,K)}) \quad (5)$$

The function is shown in Fig. 4.

Low temperature specific heat data for $Ni_{0.5}Ti_{0.5}$ were measured by Gorbunov et al. [27] and they obtained a value of 26.37 J/(K mol) at 298.15 K. Extrapolation of the fit to our data, Eq. (5), down to 298.15 K gives a value of 24.21 J/(K mol), which could be considered as good agreement.

3.3. XRD, DTA and heat content results for Al–Ni–Ti compounds

XRD and DTA were used to characterize the Al–Ni–Ti ternary compounds. XRD was used to verify that the synthesized alloys were the desired compounds. DTA was used to determine if any phase transformation occurred in the temperature range of the heat content measurement as these could produce a discontinuity in the heat content function.

The XRD results are shown in Fig. 5 and show that the alloys are single phase corresponding to the desired compounds.

DTA scans were used to determine if any phase transformations occur in the experimental temperature range for the ternary compounds, as shown in Fig. 6. Pure silver was used for calibration in the reference crucible. On heating, the silver melting appears as an exothermic peak near 1230 K, the melting point of silver. However, on cooling it appears at lower temperatures due to undercooling. There is also a heat flow change at 1173 K which corresponds to a programmed change in the heating rate. The DTA scans indicate no phase transformations for the $Al_{0.45}Ni_{0.50}Ti_{0.05}$ up to 1703 K. This is actually in contradiction with phase diagram calculation results by using a thermodynamic database [20], which shows that the $L2_1$ phase coexists with the B2 phase from room temperature up to 1573 K, above which only the B2 phase is stable and it melts at 1902 K. The discrepancy suggests that we have probably retained the B2 structure metastably down to low temperatures via quenching or the database might need improvement. For the $Al_{0.25}Ni_{0.50}Ti_{0.25}$, a small endothermic peak was observed on heating around 1513 K. This corresponds to the

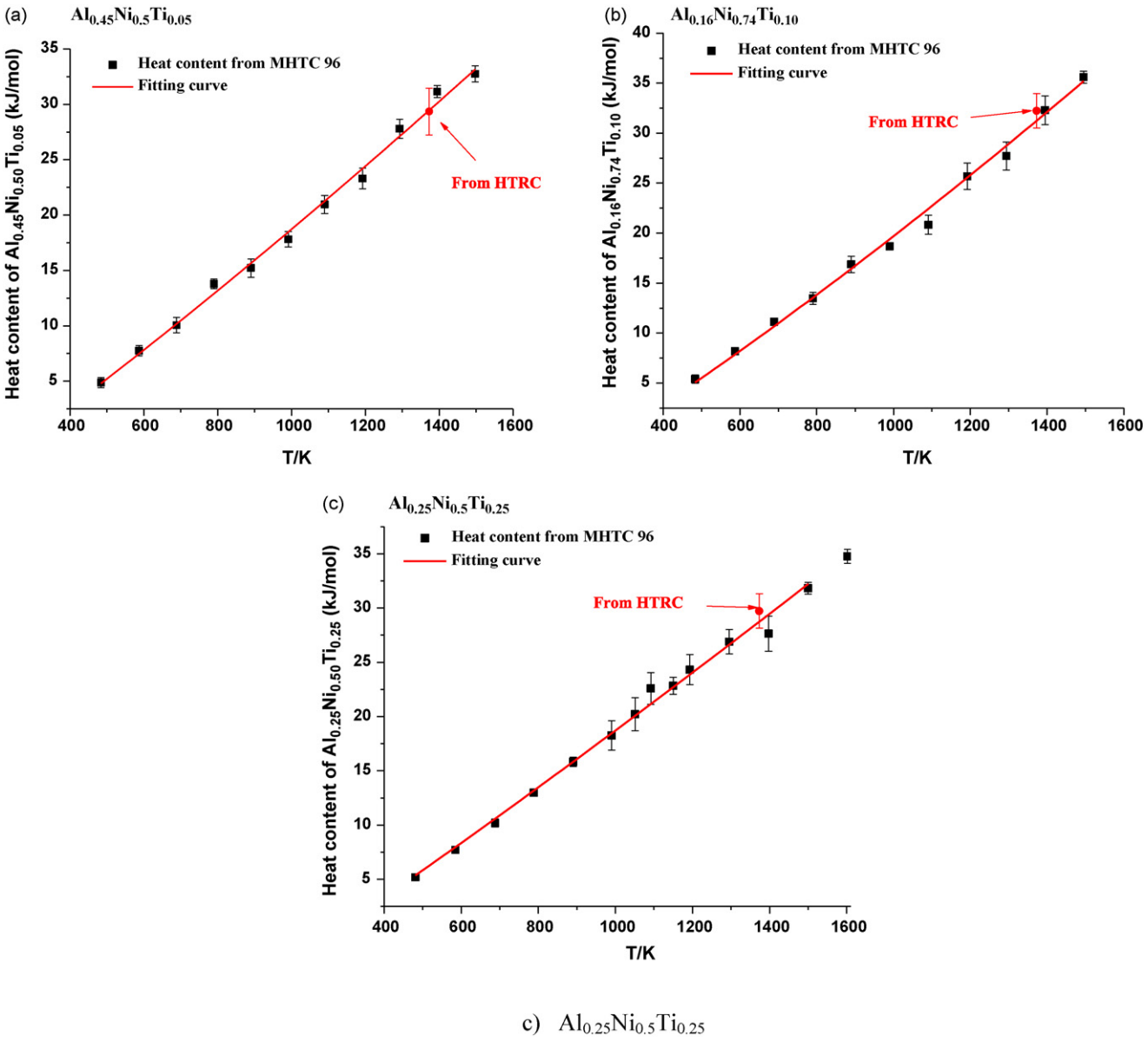

c) $Al_{0.25}Ni_{0.5}Ti_{0.25}$

Fig. 7. Molar heat content of (a) $Al_{0.45}Ni_{0.50}Ti_{0.05}$, (b) $Al_{0.16}Ni_{0.74}Ti_{0.10}$ and (c) $Al_{0.25}Ni_{0.50}Ti_{0.25}$.

melting of a few percent of eutectic phase present in this sample which was observed metallographically but not by XRD. This observation is found in fair agreement with results from a Scheil solidification simulation performed on this alloy by using the database [20], which indicates a monovariant eutectic reaction $L \rightarrow L2_1 + B2$ from 1528 to 1373 K in the end of the solidification. The calculated melting temperature for this alloy is 1771 K. In our fitting to the heat content data, we did not include the last data point at 1612 K since it is above 1513 K. For $Al_{0.16}Ni_{0.74}Ti_{0.10}$, there is significant melting starting around 1637 K on heating; however, no phase transformation occurs during the temperature range for heat content measurement (400–1495 K). The observed melting temperature for this alloy is very close to the calculated one, 1633 K, by using Dupin's Ni-based thermodynamic database [20].

The heat content of $Al_{0.45}Ni_{0.5}Ti_{0.05}$, $Al_{0.16}Ni_{0.74}Ti_{0.10}$ and $Al_{0.25}Ni_{0.5}Ti_{0.25}$ were determined using the drop calorimetry method described above, and the results are shown in Fig. 7(a–c). The highest temperature data point in Fig. 7(c) was not used for the fit as explained in Section 3.3.

The heat content values determined from the Kleppa calorimeter (HTRC) at 1373 K are also shown on the plots in Fig. 7. They are in good agreement with the results from the MHTC 96. The heat content data were fit to an equation of the form $\Delta H = A + 3R\Theta_E(1/e^{\Theta_E/T} - 1) + (b/2)T^2$ and the results for each compound, shown in Fig. 7(a–c), were as follows:

$$\text{For } Al_{0.45}Ni_{0.5}Ti_{0.05}, \quad \Delta H = 3R \times 348 \times 10^{-3} \frac{1}{\exp(348/T) - 1} + 1.71 \times 10^{-6}T^2 - 3.83\,(\text{kJ/mol}) \quad (6)$$

$$\text{For } Al_{0.16}Ni_{0.74}Ti_{0.10}, \quad \Delta H = 3R \times 351 \times 10^{-3} \frac{1}{\exp(351/T) - 1} + 2.63 \times 10^{-6}T^2 - 3.75\,(\text{kJ/mol}) \quad (7)$$

$$\text{For } Al_{0.25}Ni_{0.5}Ti_{0.25}, \quad \Delta H = 3R \times 347 \times 10^{-3} \frac{1}{\exp(347/T) - 1} + 8.88 \times 10^{-6}T^2 - 3.03(\text{kJ/mol}) \quad (8)$$

Table 1
Heat capacity fit for Al–Ni–Ti compound.

Compound	Phase	Temperature range (K)	$C_p = a + bT + c/T^2 + dT^2$ (J/(mol K))				
			a	6×10^3	$c \times 10^{-5}$	$d \times 10^6$	
			27.98				
			23.01	5.12			selected fit
$Al_{0.45}Ni_{0.5}Ti_{0.05}$	B2	484–1497	12.4	13.1	20.28		
			32.88	−17.02		11.55	
			−153	260	21.48	−95.4	
$Al_{0.5}Ni_{0.5}$	B2	500–1500	20.92	6.91			[19]
$Al_{0.25}Ni_{0.5}Ti_{0.25}$	$L2_1$	481–1602	26.41				
			25.38	1.088			selected fit
			54.45	−20	−186.5		
			6.9	43.6		−22.4	
			36.9	5.5	−41.67	−10.14	
$Ni_{0.5}Ti_{0.5}$	B2	485–1394	29.6				
			22.39	8.24			selected fit
			33.3	0.096	−26.87		
			20.0	12.54			
			52.35	120	73.58	−49.5	
$Al_{0.16}Ni_{0.74}Ti_{0.10}$	$L1_2$	483–1495	28.24				
			18.36	10.76			selected fit
			−9.57	40	62.2		
			58.55	−78.6		46.5	
			−50.99	100	11.06	−23.76	

The same approach is used for the Einstein temperature for the above compounds with use of a Debye temperature of 424 K for Al. The corresponding heat capacities were determined by differentiating Eqs. (6)–(8) resulting in the following expressions:

$$\text{For } Al_{0.45}Ni_{0.5}Ti_{0.05}, \quad C_p = 3R\left(\frac{348}{T}\right)^2 \frac{\exp(348/T)}{(\exp(348/T)-1)^2} + 3.42 \times 10^{-3} T \,(\text{J/(mol K)}) \tag{9}$$

$$\text{For } Al_{0.16}Ni_{0.74}Ti_{0.10}, \quad C_p = 3R\left(\frac{351}{T}\right)^2 \frac{\exp(351/T)}{(\exp(351/T)-1)^2} + 5.26 \times 10^{-3} T(\text{J/(mol K)}) \tag{10}$$

$$\text{For } Al_{0.25}Ni_{0.5}Ti_{0.25}, \quad C_p = 3 \times 8.314\left(\frac{347}{T}\right)^2 \frac{\exp(347/T)}{(\exp(347/T)-1)^2} + 1.776 \times 10^{-2} T(\text{J/(mol K)}) \tag{11}$$

3.4. Fitting with polynomial model

Heat capacity is commonly expressed in the following form [19]:

$$C_p = a + bT + \frac{c}{T^2} + dT^2 \tag{12}$$

and depending on the substance and accuracy of the data some parameters may be set to zero. Correspondingly, the heat content is

$$\Delta H = I + aT + \frac{b}{2}T^2 - cT^{-1} + \frac{d}{3}T^3 \tag{13}$$

The physical meaning for each term and constant was described in [28], including the lattice vibration, electronic and vacancy contributions.

The heat capacity may be expressed as

$$C_p = C_{\text{har}} + \left[\frac{2\pi^2}{3} N_A N(E_F) k^2 + 3\beta\gamma_G R\right] T + N_A k_B \exp\left\{\frac{S_{\text{vac}}}{k_B}\right\} \frac{E_{\text{vac}}^2}{k_B^2} \exp\left\{-\frac{E_{\text{vac}}}{k_B T}\right\} T^{-2} + \frac{2\pi^2}{3} N_A N(E_F) k^2 \beta\gamma_G T^2 + \beta\gamma_G N_A k_B \exp\left\{\frac{S_{\text{vac}}}{k_B}\right\} \frac{E_{\text{vac}}^2}{k_B^2} \exp\left\{-\frac{E_{\text{vac}}}{k_B T}\right\} T^{-1} \tag{14}$$

C_{har} is the harmonic lattice vibration contribution; N_A, R, k_B are Avogadro, gas and Boltzman constants; β is the cubic expansion coefficient; γ_G is the thermodynamic Grüneisen parameter; $N(E_F)$ is the electron density of states at the Fermi level; E_{vac}, S_{vac} are the formation enthalpy and entropy of vacancy, respectively.

Grimvall [28] fitted the heat capacity with an equation of the following form:

$$C_p = a + bT + cT^{-2} + dT^2 + eT^{-1} \tag{15}$$

In this work, different numbers of terms were used to fit the heat content data followed by differentiation to obtain the C_p equation. The results are listed in Table 1.

An example of the heat capacity functions obtained for $Al_{0.16}Ni_{0.74}Ti_{0.10}$ by using different numbers of terms is shown in Fig. 8. As can be seen from Table 1 and Fig. 8, fits to the data with more than two terms leads to physically unrealistic parameter values and functional behavior. Since the electronic contribution and low-order anharmonic corrections are linear in T [29], $C_p = a + bT$ was selected as the fit for these compounds. Table 1 also shows that the heat capacity of $Al_{0.45}Ni_{0.5}Ti_{0.05}$ in this work is very close to that of $Al_{0.5}Ni_{0.5}$ from [19] and in agreement with measurements from [30,31,32], seen Fig. 9.

The results show that the vacancy contribution terms T^{-1} and T^{-2} are either not significant in this temperature range or are below the sensitivity of the measurements. The higher-order anharmonic vibration contribution (T^2 term) is likewise small so that it could not be effectively measured by the drop method.

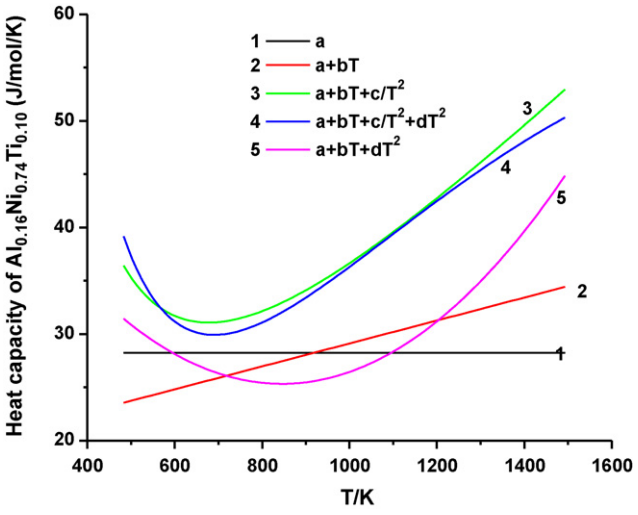

Fig. 8. Molar heat capacity of $Al_{0.16}Ni_{0.74}Ti_{0.10}$.

3.5. Heat capacity comparison

The heat content and heat capacities measured by MHTC 96 were compared with those calculated from a Ni-based superalloy database [20], as shown in Fig. 9. In Fig. 9(a′), heat capacities of $Al_{0.5}Ni_{0.5}$ from experiments [30,31,32] and a thermodynamic assessment work [33] are also added to compare with the heat capacity of $Al_{0.45}Ni_{0.5}Ti_{0.05}$, for which the $L2_1$ phase is suspended during the calculation in order to obtain metastable B2 for a meaningful comparison over the whole temperature range. The plot shows that the experimental heat capacities of $Al_{0.5}Ni_{0.5}$ and $Al_{0.45}Ni_{0.5}Ti_{0.05}$ are, as expected, very close to each other while both calculations deviate from the measurements in the same way. As a matter of fact, the experimental and calculated heat content of all alloys containing Al are not in good agreement, and the calculated heat capacities are higher than those derived from experiments and show a discontinuity around 933 K, which corresponds to the Al melting point.

Thermodynamic databases available today are all developed on the basis of the CALPHAD (CALculation of PHAse Diagrams) method [28], where multi-component phase diagrams are com-

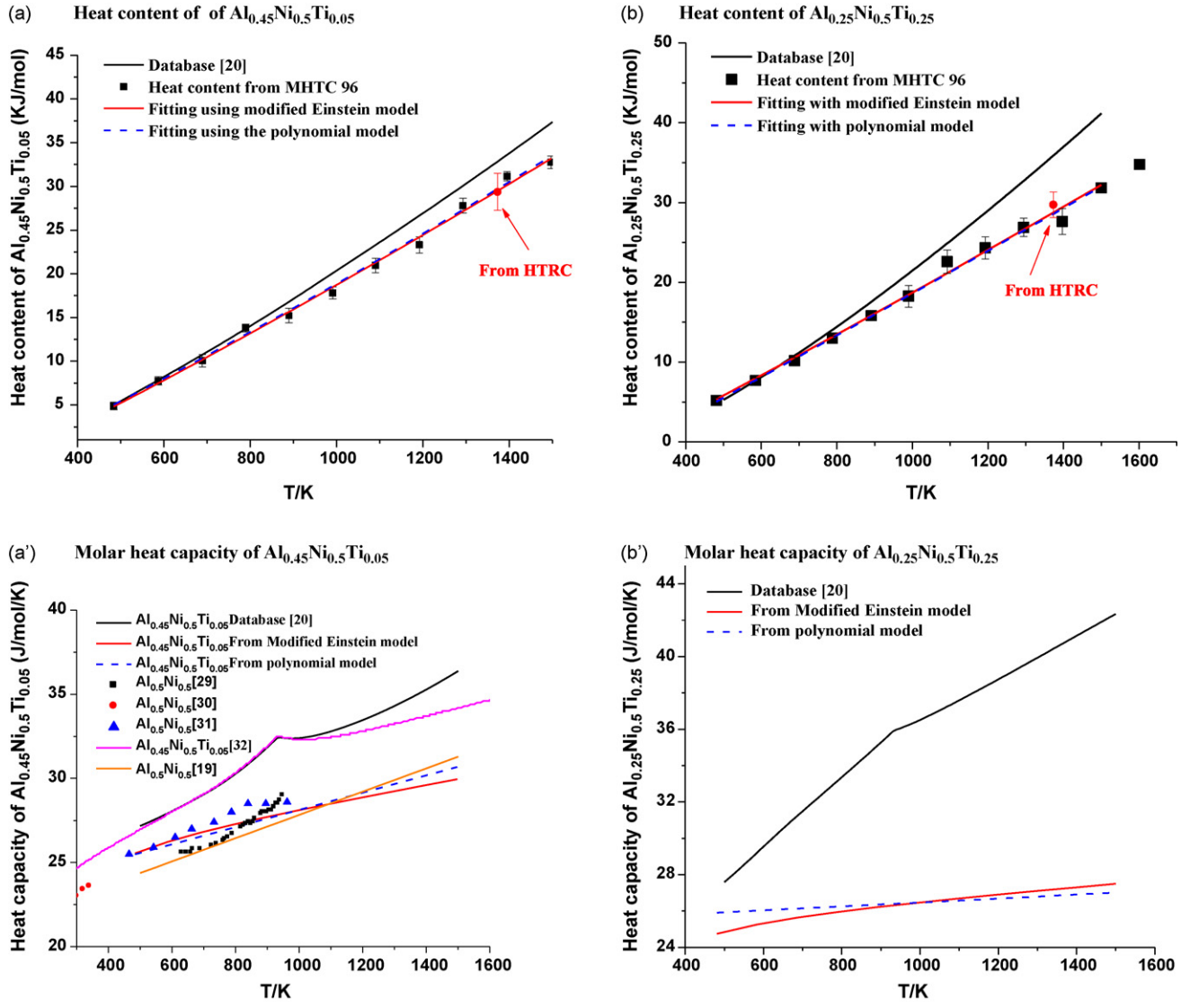

Fig. 9. Heat content and heat capacity comparison. (a) Heat content of $Al_{0.45}Ni_{0.5}Ti_{0.05}$; (a′) molar heat capacity of $Al_{0.45}Ni_{0.5}Ti_{0.05}$; (b) heat content of $Al_{0.25}Ni_{0.5}Ti_{0.25}$; (b′) molar heat capacity of $Al_{0.25}Ni_{0.5}Ti_{0.25}$; (c) heat content of $Ni_{0.5}Ti_{0.5}$; (c′) molar heat capacity of $Ni_{0.5}Ti_{0.5}$; (d) heat content of $Al_{0.16}Ni_{0.74}Ti_{0.1}$; (d′) molar heat capacity of $Al_{0.16}Ni_{0.74}Ti_{0.1}$.

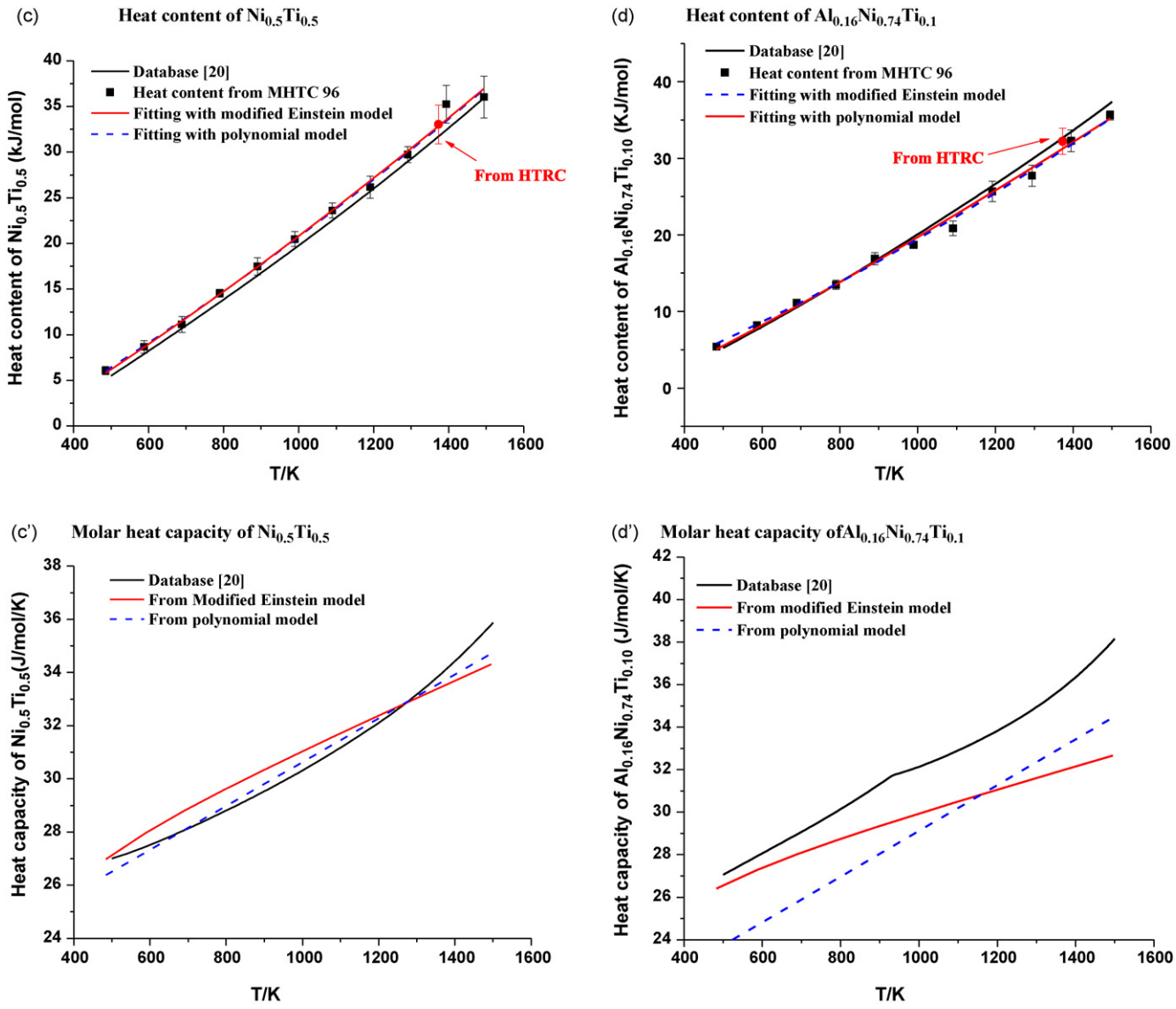

Fig. 9. (*Continued*).

puted through modeling the Gibbs energy of each individual phase. For a ternary stoichiometric compound $A_xB_yC_z$, its Gibbs energy $G_{A_xB_yC_z}$ is usually described by using a linear additive approximation:

$$G_{A_xB_yC_z} = x^0G_A^{\Phi} + y^0G_B^{\Phi} + z^0G_C^{\Phi} + a + bT \quad (16)$$

where ${}^0G_i^{\Phi}$ is the Gibbs energy of the pure element i of structure Φ, usually at the standard reference state, and a is the enthalpy of formation, b is the entropy of formation. The use of Eq. (16) implies that the Neumann-Kopp rule is applied in the description of the heat capacity of the ternary compound. As a result, features on the heat capacity curves of the pure elements will be noticeable on the curve of the compound. It is well known [34] that a simple extrapolation of the heat capacity of a pure element above its melting point may lead to unreasonable Gibbs energies that make the solid stable again at temperatures far above the melting point. In order to avoid this problem, the heat capacity for a pure solid element above its melting point is then forced to approach that of the liquid [35] in a way such as shown in Fig. 10 for Al. The kink at the melting point 933.47 K is profound and it will be kept in the thermodynamic description of alloys containing Al.

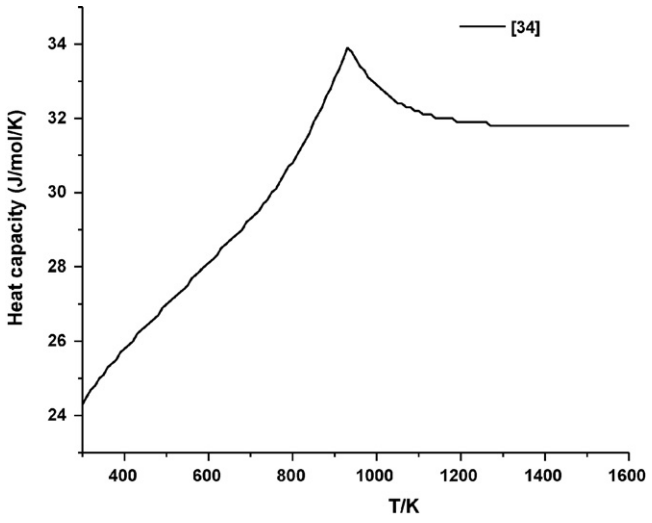

Fig. 10. Heat capacity of Al as a function of temperature from thermodynamic database [34].

Sometimes, if the experimental or theoretical information on C_p is available, the Gibbs energy of a stoichiometric compound is described just like that for a pure element by a power series in temperature [36]. In this case, no artifacts mentioned above will arise below the melting point of the compound.

For compound phases exhibiting homogeneity ranges, like the ones investigated in this work, one needs more complicated models, such as the sublattice model or compound energy formalism [35], for their Gibbs energy description, but the assumption for the heat capacities is usually the same as in Eq. (16) for the so-called end-members because it is hard to obtain information about C_p for all the end-members.

Fig. 9(a′–d′) shows that the heat capacities from the two fitting models are in reasonable agreement except for $Al_{0.16}Ni_{0.74}Ti_{0.1}$. For the three Al-containing compounds investigated in this work, the calculated heat capacities are significantly larger than the measured ones over the whole temperature range, and this suggests that the use of the Neumann-Kopp rule in thermodynamic modeling is problematic, as was also found by Huang and Chang [37] in the Al–Re system. To account for the experimental data, either a formation heat capacity term is necessary in describing the Gibbs energy of formation of the so-called end-members in the compound energy formalism or different reference states should be used.

4. Conclusions

A modified Einstein model and a polynomial model provide good representations of the heat capacity data determined from drop calorimetry experiments. The fit from both models showed that the terms from the higher-order anharmonic vibrational effects and vacancy contributions could not realistically be included in the fitting models, indicating either insufficient experimental sensitivity or the terms are very small in this temperature range relative to the first two terms. Thermodynamic databases containing Gibbs energy functions are not suitable for deriving the specific heat functions of compounds in temperature ranges where melting of one or more components occurs, unless the Gibbs energies of the compounds are not described by using the linear additive approximation.

Acknowledgements

This work is supported by the National Science Foundation under grant No. 0209624 and the International exchange program of National Natural Science Foundation of China (Grant No. 50425103). We wish to thank Professor Xiaofan Li of IIT for helpful discussions.

Appendix A. Supplementary data

Supplementary data associated with this article can be found, in the online version, at doi:10.1016/j.tca.2008.12.027.

References

[1] T. Asaoka, Mater. Sci. Res. Int. 8 (2002) 231.
[2] P.H. Kitabjian, W.D. Nix, Acta Mater. 46 (1998) 701.
[3] M.S.A. Karunaratne, P. Carter, R.C. Reed, Acta Mater. 49 (2001) 861.
[4] B. Hunean, P. Rogl, K. Zeng, R.S. Fetzer, M. Bohn, J. Bauer, Intermetallics 7 (1999) 1337.
[5] K.J. Lee, P. Nash, J. Phase Equilib. 12 (5) (1991) 551.
[6] P. Nash, W.W. Liang, Metall. Trans. A 16 (1985) 319.
[7] V. Raghavan, J. Phase Equilib. Diffus. 26 (2005) 268.
[8] J.C. Schuster, Z. Pan, S. Liu, F. Weitzer, Y. Du, Intermetallics 15 (2007) 1257.
[9] O. Kubaschewski, Trans. Faraday Soc. 54 (1958) 814.
[10] A.I. Kovalev, M.B. Bronfin, Y.V. Loshchinin, V.A. Vertogradskii, High Temp. High Press. 8 (1976) 581.
[11] R. Hu, P. Nash, Q. Chen, Enthalpy of formation of Al–Ni–Ti system, J Phase Equilib. Diffus., (2009), submitted.
[12] T. Matsui, T. Ishii, R. Sasaki, K. Naito, High Temp. High Press. 25 (1993) 531.
[13] K. Morimoto, S. Sawai, K. Hisano, Int. J. Thermophys. 20 (2) (1999) 709.
[14] K. Ishikiriyama, B. Wunderlich, J. Therm. Anal. 50 (1997) 337.
[15] Y. Arita, K. Suzuki, T. Matsui, J. Phys. Chem. Solids 66 (2005) 231.
[16] C.G. Maier, K.K. Kelley, J. Am. Chem. Soc. 54 (1932).
[17] M. Hampl, J. Leitner, K. Růžička, M. Straka, P. Svoboda, J. Therm. Anal. Calorim. 87 (2) (2007) 553.
[18] M.W. Chase, I. Ansara, G. Erikssen, G. Grimvall, L. Höglund, K. Yokokawa, Calphad 19 (4) (1995) 437.
[19] O. Kubaschewski, C.B. Alcock, P.J. Speneer, Materials Thermochemistry, 6th ed., Pergamon, Oxford, 1993, p. 258.
[20] N. Dupin, 2003, private communication.
[21] R. Hu, P. Nash, Pure Appl. Chem. (IUPAC) 79 (10) (2007) 1653.
[22] J.P. Cali, et al., National Bureau of Standard Certificate, standard reference material 781, Molybdenum—heat capacity, Washington D.C. 20234, April, 1977.
[23] Q. Chen, B. Sundman, J. Phase Equilib. 22 (6) (2001) 631.
[24] D.V. Schroeder, An Introduction to Thermal Physics, Addison-Wesley, San Francisco, CA, 2000, Section 7.5.
[25] G.B. Mitra, T. Chattopadhyay, Acta Cryst. A 28 (1972) 179.
[26] R.A. Swalin, Thermodynamics of Solids, John Wiley, New York, 1962, p. 60.
[27] V.E. Gorbunov, K.S. Gavrichev, G.A. Totrova, Z.P. Ozerova, Russ. J. Phys. Chem. 63 (6) (1989) 933.
[28] G. Grimvall, Thermophysical Properties of Materials, Elsevier, Amsterdam, 1999, p. 368.
[29] J. Kaufman, H. Bernstein, Computer Calculations of Phase Diagrams, Academic Press, New York, 1970.
[30] V.A. Troshkina, K.G. Khomyakov, Russ. J. Inorg. Chem. 6 (1961) 1233.
[31] M.I. Sandakova, V.M. Sandakov, G.I. Kalishevich, P.V. Geld, Russ. J. Phys. Chem. 45 (1971) 901.
[32] L.A. Kucherenko, V.A. Troshkina, Russ. Metall. 1 (1971) 115.
[33] Y. Du, N. Clavaguera, J. Alloys Compd. 20 (1996) 237.
[34] J.-O. Andersson, A.F. Guillermet, P. Gustafson, M. Hillert, B. Jansson, B. Jonsson, B. Sundman, J. Ågren, Calphad 11 (1987) 93.
[35] A.T. Dinsdale, Calphad 15 (1991) 317.
[36] H.L. Lukas, S.G. Fries, B. Sundman, Computational Thermodynamics: The Calphad Method, Cambridge University Press, Cambridge, 2007.
[37] W. Huang, Y.A. Chang, J. Phase Equilib. 19 (4) (1998) 361.